SciPost Phys. Proc. 8, 006 (2022)

Measurements and searches of Higgs boson production involving fermion couplings with the ATLAS detector

Shigeki Hirose* **on behalf of the ATLAS Collaboration**

Faculty of Pure and Applied Sciences, University of Tsukuba

* shhirose@hep.px.tsukuba.ac.jp

Proceedings for the XXVIII International Workshop on Deep-Inelastic Scattering and Related Subjects, Stony Brook University, New York, USA, 12-16 April 2021
doi:10.21468/SciPostPhysProc.8

Abstract

In the standard model, fermions acquire the mass via the Yukawa interaction. This mechanism can be tested by measuring couplings of the fermions with the Higgs boson. At the ATLAS experiment, the Higgs-fermion coupling measurements became possible thanks to the abundant dataset: the integrated luminosity of 139 fb^{-1} at the centre-of-mass energy of 13 TeV as well as 25 fb^{-1} at 7–8 TeV. This paper presents recent results from measurements of the Higgs boson productions in decays to a fermion pair in the final state with the ATLAS detector.

Received 09-06-2021
Accepted 06-04-2022
Published 11-07-2022
Check for updates
doi:10.21468/SciPostPhysProc.8.006

1 Introduction

The discovery of the Higgs boson by the ATLAS and CMS Collaborations [1,2] opened possibilities of better understanding the origin of the elementary particle masses in the standard model (SM). It can be tested by measuring interactions between the elementary particles and the Higgs boson. At the ATLAS experiment [3], pp collision data of 25 fb^{-1} were collected at the centre-of-mass energy $\sqrt{s} = 7$–8 TeV provided by the Large Hadron Collider (LHC). Following the two-year shutdown period for upgrading both detector and accelerator, the Run-2 operation started in 2015 through 2018, where the collision energy was increased to $\sqrt{s} = 13$ TeV, and 139 fb^{-1} data were collected [4]. At this energy, the total production cross section of Higgs bosons was 55 pb [5]. The full Run-2 dataset collected with the ATLAS detector was equivalent to $\sim$ 8 million Higgs bosons.

Using the large statistics, ATLAS achieved observations of the processes $H \to \tau\tau$ [6], $H \to bb$ [7] as well as the Higgs boson production in association with a pair of top quarks (ttH) [8]. It then became possible to measure kinematics of the Higgs boson productions in detail. For this purpose, the simplified template cross section (STXS) was developed. The

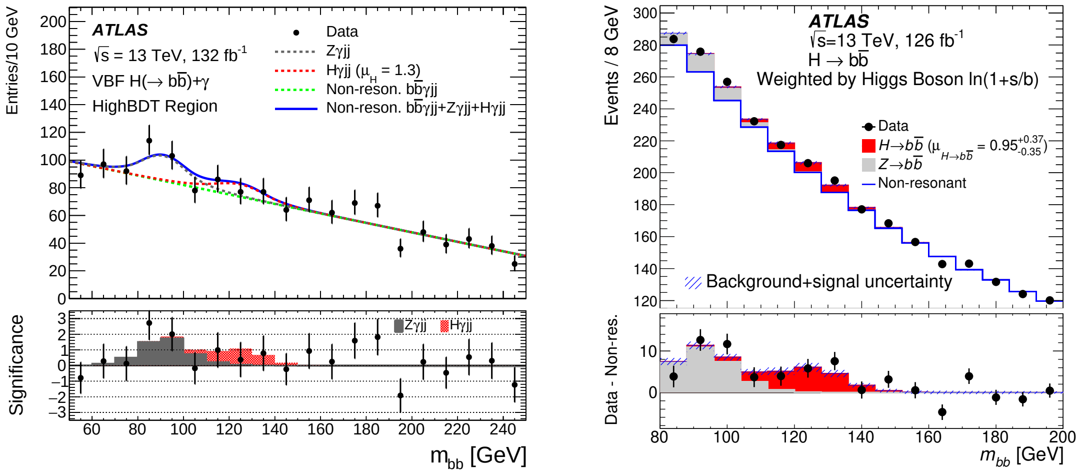

(a) (b)

Figure 1: Distributions of the bb invariant mass for two measurements of the $H \to bb$ decay with the VBF production: (a) analysis in association with an additional high energy photon [12] (only the most sensitive signal region is shown), and (b) inclusive VBF $H \to bb$ analysis [13] (events from different analysis categories are weighted depending on their respective signal-to-noise ratio). In both plots, the red (grey) histograms shows contributions from the Higgs boson signals ($Z \to bb$ background). The non-resonant backgrounds are subtracted in the bottom panels.

STXS defined regions with kinematic variables such as the number of jets, Higgs boson transverse momentum p_T^H, etc. to maximise experimental sensitivities while separating theoretically clean regions from the regions with large uncertainties [9]. It was also important that each STXS region has a sensitivity to different operators of the effective field theory. Another direction was to search for rarer processes such as $H \to \mu\mu$ and $H \to \ell\ell\gamma$. The former was in particular important for understanding of the Yukawa interaction with the second generation fermion.

In the following sections, recent results from the ATLAS experiment are presented, with emphasis on the Higgs boson production measurements with the $H \to bb$ decay (Section 2) and the rare process searches with leptonic final states (Section 3).

2 Measurements of the $H \to bb$ decay

It is challenging to measure the $H \to bb$ decay at LHC due to large background originating from multi-jet events containing b-quark jets (b-jets). Nevertheless, observation of $H \to bb$ has been achieved using the VH production process [10], where the final state involving a leptonically decaying vector boson ($Z \to \ell\ell$, $Z \to \nu\nu$ or $W \to \ell\nu$) provides a clean signature. Including a novel analysis technique reconstructing two close-by b-jets from a Higgs boson decay as a single large-radius (large-R) jet [11], the $H \to bb$ decay has been measured with the significance of nearly 7 standard deviation (σ). The STXS in seven regions depending on the vector boson species ($V = W, Z$) and its p_T have been measured with precision of 30–100% [10, 11].

The vector boson fusion (VBF) production has a cross section 65% higher than that of the VH process. It provides a cleaner signature thanks to presence of two high-p_T jets emitted to the opposite directions. However, such a multi-jet final state is challenging in efficient trigger-

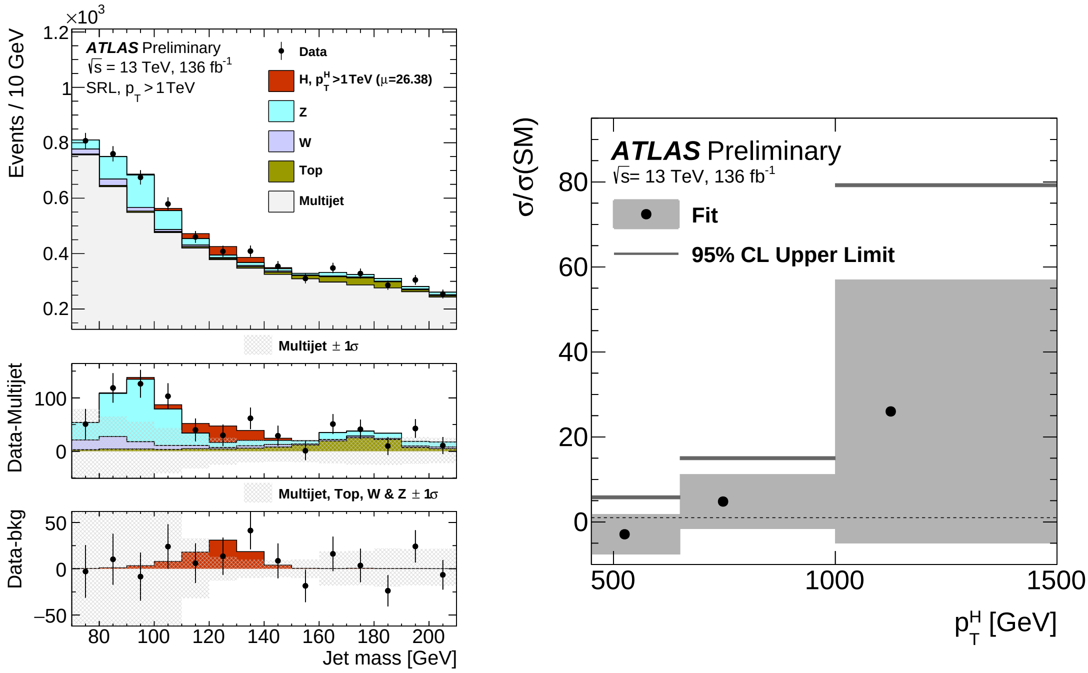

(a) (b)

Figure 2: (a) Jet-mass distribution in the signal region where the highest-p_{T} large-R jet with $p_{\mathrm{T}} > 1$ TeV has two b-tagged sub-jets [14]. The top panel shows the original mass distribution, while the middle (bottom) panel is the distribution where the multi-jet (both multi-jet and resonant) background is subtracted. (b) Results from the p_{T}^{H}-dependent cross section measurement [14].

ing. Two orthogonal measurements have been recently performed; one requires existence of an additional high energy isolated photon which can be used for the trigger [12], and more inclusive measurement with four-jet events targeting a high p_{T}^{H} Higgs boson candidates (p_{T}^{H} > 150 GeV) [13]. Figure 1 shows di-b-jet mass distributions for these two analysis. In combination, the number of VBF signals relative to that expected from the SM, or signal strength, is measured to be $\mu = 0.99 \pm 0.30(\text{stat.})^{+0.18}_{-0.16}(\text{syst.})$, corresponding to an observed significance of 2.9σ.

A more inclusive measurement is attempted, targeting very high-p_{T}^{H} Higgs boson production ($p_{\mathrm{T}}^{H} \sim 1$ TeV) [14]. Events with at least one large-R jet with two b-tagged sub-jets are chosen. Two orthogonal signal regions are defined, depending on the highest-p_{T} or the second highest-p_{T} large-R jets have two b-tagged sub-jets. Events with large-R jets but without any b-tagged sub-jets are used for modelling and validating backgrounds, such as events with multi-jets, vector bosons and top quarks. Figure 2(a) shows distribution of the jet mass of doubly b-tagged large-R jets in the most sensitive signal region. No significant signal peak is observed while background models are in good agreement with data. Figure 2(b) shows a summary of the results from the p_{T}^{H}-dependent cross section measurements. With a sizeable uncertainty, the cross section is measured up to the region $p_{\mathrm{T}}^{H} > 1$ TeV. The dominant uncertainty originates from limited data statistics, followed by the jet mass resolution.

The ttH production has been measured with several different final states [15]. While a measurement with $H \to bb$ suffers from a large background with a top-quark pair in association with additional b-jets, it has an advantage of the large branching ratio. In the previous

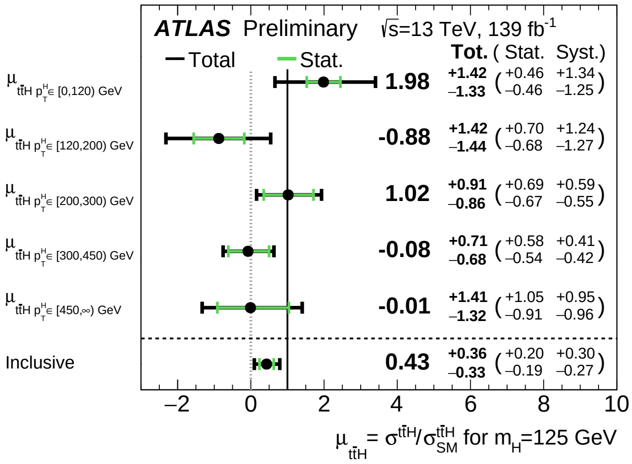

Figure 3: Measured signal strength for ttH signals in each STXS bins, as well as the inclusive signal strength [17].

measurement based on a partial dataset of Run 2 [16], the result was dominated by systematic uncertainties arising from modelling of background distributions containing a top-quark pair. In the updated measurement with the full Run-2 dataset [17], five control regions are defined to well control the background. Signal events are categorised into 11 regions motivated by the STXS. Figure 3 shows the measured μ for each STXS region, where all results are consistent with the SM expectations. This is the first STXS measurement for the ttH process. The inclusive result is $\mu = 0.43 \pm^{+0.20}_{-0.19}$ (stat.)$^{+0.30}_{-0.27}$(syst.), corresponding to the observed significance of 1.3σ while 3.0σ is expected.

3 Searches for rare Higgs boson decays with leptonic final states

Higgs boson decays with leptonic final states typically have cleaner signatures compared with hadronic final states, thanks to absence of the strong interaction in the final-state leptons. For example, the $H \to \tau\tau$ decay is a well-established channel with the uncertainly better than 20% [18] on signal strength. Using the cleaner signatures, rarer channels with light leptons such as $H \to \mu\mu$ are possible to access, regardless their small branching ratio at $O(10^{-4})$.

The $H \to \mu\mu$ decay is an important channel to test the Yukawa interaction with the second-generation fermions. Although the final state composed of a pair of oppositely-charged high-p_{T} isolated muons is clean, the measurement is suffered from a large $Z^{(*)}/\gamma^* \to \mu\mu$ background. In the latest measurement [19], to separate signals from the background as efficiently as possible, the resolution of the di-muon mass distribution is improved by adding up to one final-state radiation photon into the mass reconstruction. Events are categorised into 20 orthogonal signal regions based on output classifiers of the boosted decision tree trained with jet and muon kinematics. The obtained result is $\mu = 1.2 \pm 0.6$(stat.)$^{+0.2}_{-0.1}$(syst.), which corresponds to an observed significance of 2.0σ, and is consistent with the SM expectation. In combination with the result from the CMS Collaboration [20], an evidence of the $H \to \mu\mu$ decay is observed for the first time.

The $H \to \ell\ell\gamma$ decay is a process via a loop with mainly heavy particles such as a top quark and a weak boson, emitting one real photon and another virtual Z or γ decaying into a pair of light leptons. With a di-lepton mass ($m_{\ell\ell}$) less than 30 GeV, a contribution from a virtual photon is dominant. This process provides a complementary information of couplings

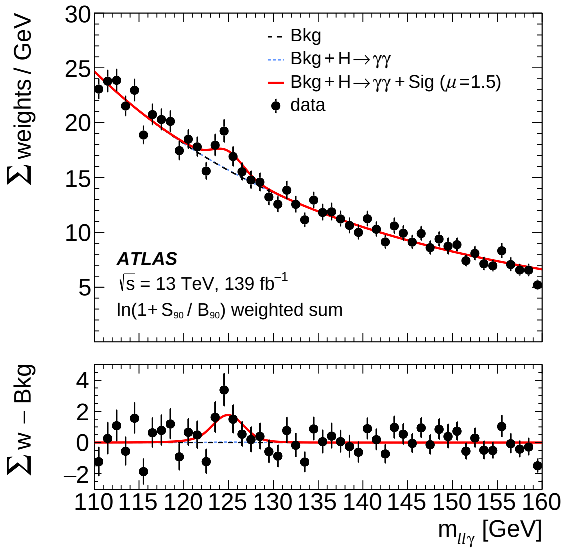

Figure 4: Distribution of $m_{\ell\ell\gamma}$, where events from different analysis categories are weighted depending on their signal-to-noise ratio [21].

between H and intermediate particles with respect to the direct coupling measurements. In the latest measurement [21], events are categorised based on the lepton flavour (ee or $\mu\mu$) and kinematics (VBF topology, high-p_T and low-p_T). In the electron channel, events with a small $m_{\ell\ell}$ have a narrow opening angle, resulting in a merged cluster in the calorimeter. The analysis is therefore designed to allow events with a larger calorimeter cluster having two associated charged tracks to retain. Figure 4 shows the invariant mass distribution formed with a di-lepton and a photon ($m_{\ell\ell\gamma}$) in the signal region. The main background originates from events with non-resonant $\ell\ell\gamma$; they are modelled with an analytic function and normalised in the fit. The observed significance corresponds to 3.2σ, resulting in the first evidence of $H \to \ell\ell\gamma$.

4 Summary

Using the full Run-2 dataset, many measurements on the Higgs boson properties have been performed. The large statistics allows precision tests for the Yukawa couplings in the third-generation fermions. Those results are more and more important in the STXS measurements. Rare decays such as $H \to \mu\mu$ and $H \to \ell\ell\gamma$ becomes accessible; evidences have been obtained for these channels. More measurements as well as full combinations for the STXS measurements and their interpretations in terms of the effective field theory are ongoing. In the LHC Run-3 operation, the data size will be doubled; therefore it provides opportunities to more precisely understand the Higgs boson properties.

References

[1] ATLAS Collaboration, *Observation of a new particle in the search for the Standard Model Higgs boson with the ATLAS detector at the LHC*, Phys. Lett. B **716**, 1 (2012), doi:10.1016/j.physletb.2012.08.020.

[2] CMS Collaboration, *Observation of a new boson at a mass of 125 GeV with the CMS experiment at the LHC*, Phys. Lett. B **716**, 30 (2012), doi:10.1016/j.physletb.2012.08.021.

[3] ATLAS Collaboration, *The ATLAS Experiment at the CERN Large Hadron Collider*, J. Inst. **3**, S08003 (2008), doi:10.1088/1748-0221/3/08/S08003.

[4] ATLAS Collaboration, *ATLAS data quality operations and performance for 2015–2018 data-taking*, J. Inst. **15**, P04003 (2020), doi:10.1088/1748-0221/15/04/P04003.

[5] D. de Florian et al., *Handbook of LHC Higgs Cross Sections: 4. Deciphering the Nature of the Higgs Sector*, CERN Yellow Reports: Monographs. CERN, Geneva (2016), doi:10.23731/CYRM-2017-002.

[6] ATLAS Collaboration, *Evidence for the Higgs-boson Yukawa coupling to tau leptons with the ATLAS detector*, J. High Energy Phys. **04**, 117 (2015), doi:10.1007/JHEP04(2015)117.

[7] ATLAS Collaboration, *Observation of $H \to b\bar{b}$ decays and VH production with the ATLAS detector*, Phys. Lett. B **786**, 59 (2018), doi:10.1016/j.physletb.2018.09.013.

[8] ATLAS Collaboration, *Observation of Higgs boson production in association with a top quark pair at the LHC with the ATLAS detector*, Phys. Lett. B **784**, 173 (2018), doi:10.1016/j.physletb.2018.07.035.

[9] N. Berger et al., *Simplified Template Cross Sections - Stage 1.1*, arXiv:1906.02754.

[10] ATLAS Collaboration, *Measurements of WH and ZH production in the $H \to b\bar{b}$ decay channel in pp collisions at 13 TeV with the ATLAS detector*, Eur. Phys. J. C **81**, 178 (2021), doi:10.1140/epjc/s10052-020-08677-2.

[11] ATLAS Collaboration, *Measurement of the associated production of a Higgs boson decaying into b-quarks with a vector boson at high transverse momentum in pp collisions at $\sqrt{s}$ = 13 TeV with the ATLAS detector*, Phys. Lett. B **816**, 136204 (2021), doi:10.1016/j.physletb.2021.136204.

[12] TLAS Collaboration, *Search for Higgs boson production in association with a high-energy photon via vector-boson fusion with decay into bottom quark pairs at $\sqrt{s}$=13 TeV with the ATLAS detector*, J. High Energy Phys. **03**, 268 (2021), doi:10.1007/JHEP03(2021)268.

[13] ATLAS Collaboration, *Measurements of Higgs Bosons Decaying to Bottom Quarks from Vector Boson Fusion Production with the ATLAS Experiment at $\sqrt{s}$ = 13 TeV*, Eur. Phys. J. C **81**, 537 (2021), doi:10.1140/epjc/s10052-021-09192-8.

[14] ATLAS Collaboration, *Study of Higgs-boson production with large transverse momentum using the $H \to b\bar{b}$ decay with the ATLAS detector*, ATLAS-CONF-2021-010 (2021).

[15] ATLAS Collaboration, *A combination of measurements of Higgs boson production and decay using up to 139 fb^{-1} of proton–proton collision data at $\sqrt{s}$ = 13 TeV collected with the ATLAS experiment*, ATLAS-CONF-2020-027 (2020).

[16] ATLAS Collaboration, *Search for the standard model Higgs boson produced in association with top quarks and decaying into a $b\bar{b}$ pair in pp collisions at $\sqrt{s}$ = 13 TeV with the ATLAS detector*, Phys. Rev. D **97**, 072016 (2018), doi:10.1103/PhysRevD.97.072016.

[17] ATLAS Collaboration, *Measurement of the Higgs boson decaying to b-quarks produced in association with a top-quark pair in pp collisions at $\sqrt{s}$ = 13 TeV with the ATLAS detector*, ATLAS-CONF-2020-058 (2020).

[18] ATLAS Collaboration, *Cross-section measurements of the Higgs boson decaying into a pair of τ-leptons in proton-proton collisions at $\sqrt{s}$ = 13 TeV with the ATLAS detector*, Phys. Rev. D **99**, 072001 (2019), doi:10.1103/PhysRevD.99.072001.

[19] ATLAS Collaboration, *A search for the dimuon decay of the Standard Model Higgs boson with the ATLAS detector*, Phys. Lett. B **812**, 135980 (2021), doi:10.1016/j.physletb.2020.135980.

[20] CMS Collaboration, *Evidence for Higgs boson decay to a pair of muons*, J. High Energy Phys. **01**, 148 (2021), doi:10.1007/JHEP01(2021)148.

[21] ATLAS Collaboration, *Evidence for Higgs boson decays to a low-mass dilepton system and a photon in pp collisions at $\sqrt{s} = 13$ TeV with the ATLAS detector*, Phys. Lett. B **819**, 136412 (2021), doi:10.1016/j.physletb.2021.136412.